REMOTE SENSING OF ENVIRONMENT 15:119–133 (1984)

Calculations of Radar Backscattering Coefficient of Vegetation-Covered Soils

TSAN MO

Computer Sciences Corporation, Silver Spring, Maryland 20910

THOMAS J. SCHMUGGE

Hydrological Sciences Branch, Code 924, NASA/Goddard Space Flight Center, Greenbelt, Maryland 20771

and

THOMAS J. JACKSON

USDA/ARS Hydrology Laboratory, Beltsville, Maryland 20705

A model for simulating the measured radar backscattering coefficient of vegetation-covered soil surfaces is presented in this study. The model consists of two parts: the first is a soil surface model to describe the backscattered radar pulses from a rough soil surface, and the second part takes into account the effect of vegetation cover. The soil surface is characterized by two parameters, the surface height standard deviation σ and the horizontal correlation length l. The effect of vegetation canopy scattering is incorporated into the model by making the radar pulse subject to two-way attenuation and volume scattering when it passes through the vegetation layer. These processes are characterized by the two parameters, the canopy optical thickness τ and the volume scattering factor η. The model results agree well with the measured angular distributions of the radar backscattering coefficient for HH polarization at the 1.6 GHz and 4.75 GHz frequencies over grass-covered fields. These observations were made from an aircraft platform during six flights over a grass watershed in Oklahoma. It was found that the coherent scattering from soil surfaces is very important at angles near nadir, while the vegetation volume scattering is dominant at larger incident angles (> 30°). The results show that least-squares fits to scatterometer data can provide reliable estimates of the surface roughness parameters, particularly the surface height standard deviation σ. The range of values for σ for the six flights is consistent with a 2 or 3 dB uncertainty in the magnitude of the radar response.

Introduction

Recently, there have been many microwave radar measurements made of Earth terrain under various surface conditions (Jackson et al., 1980; 1982; Theis et al., 1982a; 1982b; Ulaby, 1978; 1981; Allen et al., 1982; Attema and Ulaby, 1978). These measurements were usually taken with either truck-mounted or airborne scatterometers at various frequencies, and the resulting data are in the form of radar backscattering coefficients $\sigma^0(\theta)$, which are expressed in units of decibels (dB) as a function of incidence angle θ. Analysis of the measured radar backscattering coefficients can provide valuable information about the surface soil moisture content, roughness parameters of the soil surface, and the vegetation cover. Theoretical simulations of the data can increase our understanding of the manner in which microwave radiation is backscattered from multilayer media (such as from vegetation-covered soils). Several theoretical models (Tsang et al., 1982; Stogryn, 1967; Fung and Eom, 1981a; 1981b; Semyonov, 1966; Ulaby et al.,

52 Vanderbilt Ave., New York, NY 10017 0034-4257/84/$3.00

1982) have been developed to simulate the backscattering process, and they provide an excellent means of describing the returned radar signals to the scatterometers. However, the theoretical models are usually complicated and have many parameters, values of which are difficult, if not impossible, to obtain over large natural or agricultural fields. From an experimentalist's viewpoint, it would be desirable to have a simple model with a parametric description of the scattering media with the minimum number of parameters necessary to interpret the measured backscattering coefficients.

The present study was undertaken to develop a simple "user's" model for simulating the measured radar backscattering coefficients from vegetation-covered fields in conjunction with the data obtained by Jackson et al. (1980; 1982). The model is based on the theoretical work by Fung and Eom (1981a), but modified to include the effect of a vegetation canopy. In addition, the Fresnel reflectivity which appears in the model (Fung and Eom, 1981a) was replaced by calculated soil surface reflectivity which was obtained from a radiative transfer model (Wilheit, 1978), using measured profiles of soil moisture and temperature. The model consists of two parts: the first is a soil surface model to describe the scatter from rough, bare soil, and the second part takes into account the effect of a vegetation cover. There are four parameters: two of these parameters, which are used in the soil surface model, specify the condition of the soil surface (the surface height standard deviation σ and the correlation length l), and the other two define the characteristics of the canopy (the canopy optical thickness τ and the canopy volume scattering factor η).

Comparison of the model calculations with the measured radar backscattering coefficients at the frequencies 1.6 GHz (L-band) and 4.75 GHz (C-band) over grass-covered fields shows good agreement. The model calculations demonstrate that the large magnitudes of the measured $\sigma^0(\theta)$ at angles close to nadir are primarily due to the coherent scattering from soil surface and that the $\sigma^0(\theta)$ values at large incident angles ($\theta > 30°$) can be attributed to vegetation canopy scattering. The incoherent scattering contributes to the backscattering coefficient at all angles for a rough soil surface.

The Model

A radar pulse reflected from a vegetation-covered soil surface is subject to two-way attenuation and scattering by the vegetation layer, as shown schematically in Fig. 1. We assume that the geometrical configuration is symmetric with respect to the azimuth angle ϕ and that Fig. 1 corresponds to the $\phi = 0$ case. Backscattering occurs at $\theta_s = \theta$, $\phi_s = \pi$, and $\phi = 0$, where (θ, ϕ) denote the incident direction and (θ_s, ϕ_s) the scattered direction.

The backscattering coefficient $\sigma^0(\theta)$ of vegetation-covered soils can be written in the form (Attema and Ulaby, 1978; Tsang et al., 1982)

$$\sigma^0(\theta) = \sigma_v^0(\theta) + \sigma_s^0(\theta) e^{-2\tau/\cos\theta}, \quad (1)$$

where $\sigma_v^0(\theta)$ is the vegetation backscattering coefficient, $\sigma_s^0(\theta)$ is the soil backscattering coefficient, and τ is the optical thickness of the vegetation layer. Following previous investigations (Attema and Ulaby, 1978; Tsang et al., 1982), the

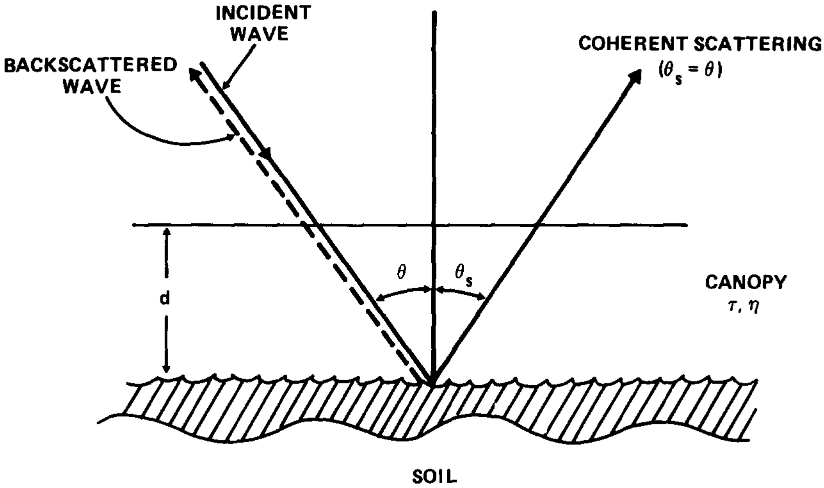

FIGURE 1. Schematic view of the scattering geometry. The θ and θ_s represent the incident and scattered angles, respectively. The thickness of the vegetation layer is denoted by d.

vegetation scattering component $\sigma_v^0(\theta)$ can be approximated by

$$\sigma_v^0(\theta) = \frac{\eta \cos\theta}{2\tau}\left(1 - e^{-2\tau/\cos\theta}\right), \quad (2)$$

where η, which depends on the canopy water content per unit area (Attema and Ulaby, 1978), is a vegetation volume scattering factor.

For a rough soil surface, the backscattering coefficient $\sigma_s^0(\theta)$ consists of two components: the coherent backscattering coefficient $\sigma_{\mathrm{coh}}^0(\theta)$ and the incoherent backscattering coefficient $\sigma_{\mathrm{inc}}^0(\theta)$. The coherent scattering component $\sigma_{\mathrm{coh}}^0(\theta)$ occurs only in the specular direction (i.e., $\theta_s = \theta$), and thus a monostatic radar would not receive any return power from the coherent scattering component except for normal incidence (Ulaby et al., 1982). However, a radar with finite beamwidth antenna pattern can receive both coherent and incoherent scatterings, particularly near the nadir direction.

Thus, one can write the $\sigma_s^0(\theta)$ in the form

$$\sigma_s^0(\theta) = \sigma_{\mathrm{coh}}^0(\theta) + \sigma_{\mathrm{inc}}^0(\theta). \quad (3)$$

The coherent scattering of microwave waves from a rough soil surface has been investigated by several authors (Fung and Eom, 1981a; Tsang and Newton, 1982).

The general form, as a function of both incident and scattered angles, can be given by (Fung and Eom, 1981a; Tsang and Newton, 1982),

$$\sigma_{\mathrm{coh}}^0(\theta, \phi; \theta_s, \phi_s) = \pi k^2 |a_0|^2 \delta(q_x)\,\delta(q_y) e^{-q_z^2 \sigma^2}, \quad (4)$$

where k is the wave number of the incident wave, δ is the Dirac delta function, and σ is the standard deviation of the surface height. The quantities q_x, q_y, q_z, and a_0 are defined as (Fung and Eom, 1981a; Ulaby et al., 1982)

$$\begin{aligned}
q_x &= k(\sin\theta_s\cos\phi_s - \sin\theta\cos\phi),\\
q_y &= k(\sin\theta_s\sin\phi_s - \sin\theta\sin\phi),\\
q_z &= k(\cos\theta_s + \cos\theta) \qquad (5)\\
a_0 &= |R_{\mathrm{pp}}|(\cos\theta + \cos\theta_s)\cos(\phi_s - \phi)\\
&\qquad (\mathrm{pp} = \mathrm{HH\ or\ VV}).
\end{aligned}$$

The delta functions in Eq. (4) limit the coherent scattering to the specular direction, $\theta_s = \theta$ and $\phi_s = \phi$. The magnitude of this coherent scattering along the specular direction can be obtained by integrating Eq. (4) across the $\theta_s = \theta$ and $\phi_s = \phi$ direction of the scattered solid angle $d\Omega_s = d\cos\theta_s\, d\phi_s$, and the result is approximated by $\sigma^0_{\mathrm{coh}}(\theta)$, i.e.,

$$\begin{aligned}
\sigma^0_{\mathrm{coh}}(\theta) &= \int_{\Delta\Omega_s} \sigma^0_{\mathrm{coh}}(\theta,\phi;\theta_s,\phi_s)\, d\Omega_s\\
&= 4\pi|R_{\mathrm{pp}}|^2\cos\theta\, e^{-h\cos^2\theta}, \qquad (6)
\end{aligned}$$

where $h = 4k^2\sigma^2$ and the quantity $|R_{\mathrm{pp}}|^2$ represents the reflectivity of a smooth surface.

The coherent backscattering coefficient $\sigma^0_{\mathrm{coh}}(\theta)$ defined in Eq. (6) corresponds to a monochromatic radar beam. In practice, a radar has a transmitting antenna pattern with a finite beamwidth, and thus the actual coherent backscattering coefficient is distributed according to the transmitting antenna pattern $G_t(\theta)$. Also the received radar power is determined by the receiving antenna pattern $G_r(\theta')$ for a returned coherent beam located at an angle θ', measured from the center of the antenna beam.

Assume that the product of the antenna gain patterns is represented by the Gaussian form,

$$\begin{aligned}
f(\theta) &= G_t(\theta)G_r(\theta)\\
&= \exp\left[-a(\theta-\theta_0)^2/\beta^2\right], \qquad (7)
\end{aligned}$$

where β is the 3-dB antenna beamwidth and $a = 4\ln 2$. The angle θ_0 is the location of the center of the antenna beam.

Since coherent scattering occurs only in the specular direction (see Fig. 1), the functional form of receiving antenna gain pattern for coherent scattering can be obtained from the one given in Eq. (7) by changing $(\theta - \theta_0)$ to $(\theta + \theta_0)$. The returned coherent scattering at an angle $\theta' = \theta + \theta_0$ can make contributions to the measured backscattering coefficient through an appropriate "coherent" antenna gain pattern, which can be approximated by

$$\begin{aligned}
g_c(\theta) &= G_t(\theta)G_r(\theta')\\
&= \exp\left[-a(\theta-\theta_0)^2/2\beta^2\right]\\
&\quad \times \exp\left[-a(\theta+\theta_0)^2/2\beta^2\right]\\
&= \exp\left[-a(\theta^2+\theta_0^2)/\beta^2\right]. \qquad (8)
\end{aligned}$$

Therefore, the "measureable" coherent contribution to the backscattering coefficient can be defined by the weighted quantity

$$\langle\sigma^0_{\mathrm{coh}}(\theta)\rangle = g_c(\theta)\sigma^0_{\mathrm{coh}}(\theta), \qquad (9)$$

where $\sigma^0_{\mathrm{coh}}(\theta)$ and $g_c(\theta)$ are given by Eqs. (6) and (8), respectively.

The incoherent backscattering coefficient $\sigma^0_{\mathrm{inc}}(\theta)$ in Eq. (3) depends on the statistical properties of a rough surface: the surface height standard deviation σ and the correlation length l. The latter provides a reference for estimating the statistical independence of two points on a surface (Ulaby et al., 1982). Models for $\sigma_{\text{inc}}^0(\theta)$ have been developed by many authors (Fung and Eom, 1981a; Ulaby et al., 1982; Mo, 1982; Tsang and Newton, 1982). The one developed by Fung and Eom (1981a) is relatively simple in application, and it will be further developed in this study to fit the backscattering coefficient data.

A backscattering coefficient from a rough soil surface depends on the surface correlation function of its height distribution. Both Gaussian and non-Gaussian correlation functions have been used for numerical calculations of backscattering coefficient (Fung and Eom, 1981a; Ulaby et al., 1982; Eom and Fung, 1982). For mathematical simplicity, the Gaussian form of correlation function has been widely used in the computation of the backscattering coefficient. In this study, we assume that a rough soil surface has a Gaussian surface correlation function $\rho(\xi)$ and a horizontal correlation length l, i.e.,

$$\rho(\xi)=\exp(-\xi^2/l^2), \tag{10}$$

where ξ is a distance between two points on the horizontal surface. Then following a similar process as given by Mo (1982), one can show that the incoherent backscattering coefficient $\sigma_{\text{inc}}^0(\theta)$ for pp polarization is given by the form (Fung and Eom, 1981a; Ulaby et al., 1982)

$$\begin{aligned}\sigma_{\text{inc}}^0(\theta)=(kl)^2\Big[&|R_{\text{pp}}|^2(1+\sin^2\theta)\\&+\operatorname{Re}\big(R_{\text{pp}}R_{\text{pp1}}^*\big)\sin 2\theta\Big]\\&\times e^{-h\cos^2\theta}\sum_{n=1}^{\infty}\frac{(h\cos^2\theta)^n}{n!n}\\&\times\exp\left[-\frac{(kl\sin\theta)^2}{n}\right],\end{aligned}\tag{11}$$

where $h=4k^2\sigma^2$, $|R_{\text{pp}}|^2$ denotes the smooth surface reflectivity, and R_{pp1}^* is the complex conjugate of R_{pp1}, which is a component of the reflectivity. For pp = HH, it can be related to R_{HH} by the relation (Fung and Eom, 1981a; Ulaby et al., 1982)

$$\begin{aligned}R_{\text{HH1}}=&-R_{\text{HH}}\\&\times 2\sin\theta/\left(\cos\theta+\sqrt{\varepsilon_s-\sin^2\theta}\right),\end{aligned}\tag{12}$$

where ε_s is the complex dielectric constant of soil. For other polarizations, explicit forms of R_{pp1} can be found in Fung and Eom (1981a) and Ulaby et al. (1982).

In applying Eq. (11) to the backscattering coefficient, the quantity $\sigma_{\text{inc}}^0(\theta)$ should be weighted by the antenna gain pattern $f(\theta)$ given in Eq. (7). Similar to $\langle\sigma_{\text{coh}}^0(\theta)\rangle$ in Eq. (9), one can define the quantity

$$\langle\sigma_{\text{inc}}^0(\theta)\rangle=f(\theta)\sigma_{\text{inc}}^0(\theta) \tag{13}$$

as the weighted incoherent backscattering coefficient. Therefore, the total soil backscattering coefficient $\langle\sigma_s^0(\theta)\rangle$, weighted by appropriate antenna gain patterns, can be written in the form

$$\begin{aligned}\langle\sigma_s^0(\theta)\rangle&\equiv\langle\sigma_{\text{coh}}^0(\theta)\rangle+\langle\sigma_{\text{inc}}^0(\theta)\rangle\\&=g_c(\theta)\sigma_{\text{coh}}^0(\theta)+f(\theta)\sigma_{\text{inc}}^0(\theta)\\&=f(\theta)\big[\sigma_{\text{coh}}^0(\theta)\\&\qquad\times\exp(-2a\theta\theta_0/\beta^2)+\sigma_{\text{inc}}^0(\theta)\big],\end{aligned}\tag{14}$$

where Eqs. (7) and (8) have been employed in arriving at the last step in Eq. (14).

For comparing with the data, the calculated backscattering coefficient

$\langle \sigma_s^0(\theta) \rangle$ from Eq. (14) and the vegetation backscattering coefficient $\sigma_v^0(\theta)$ from Eq. (2) should be averaged over the main beam of the antenna patterns, or, more precisely, over the illuminated target area bounded by the main antenna beam. Allen et al. (1982) have presented the detailed description of the geometrical configuration, and our final result of the weighted average total backscattering coefficient $\langle \sigma^0(\theta) \rangle_{\text{ave}}$ can be written as

$$\langle \sigma^0(\theta) \rangle_{\text{ave}} = \frac{1}{A} \int\int \left[\langle \sigma_s^0(\theta) \rangle \exp\left(\frac{-2\tau}{\cos\theta} \right) + f(\theta) \sigma_v^0(\theta) \right] \tan\theta \, d\theta \, d\phi, \tag{15}$$

where the factor $\tan\theta$ comes from the geometrical configuration of the illuminated target area (Allen et al., 1982), and the normalization factor A is given by

$$A = \int\int f(\theta) \tan\theta \, d\theta \, d\phi. \tag{16}$$

Equation (15) will be used to fit the data, as described in the next section. The ϕ integrations in Eqs. (15) and (16) can be omitted if the integrands are independent of ϕ.

The Results

The formulas derived in the previous section were used to fit the measured backscattering coefficient (Jackson et al., 1980; 1982) at L- and C-band frequencies over four different grass-covered watersheds located near Chickasha, Oklahoma in 1978 and 1980. The data for HH polarization, taken with airborne scatterometers from an altitude of 300 m, were given in decibels (dB) at incident angles between 5° and 50° at 5° increments. The soil texture of the fields is silt loams (Jackson, 1983) consisting of 35% sand, 20% clay, and 45% silt, approximately. Soil moisture profiles were measured within three depth intervals: 0–2.5 cm, 2.5–5 cm, and 5–15 cm. Also measured were the soil temperatures. These measured soil moistures and temperatures were employed to calculate the soil dielectric constant ε_s and the soil surface reflectivity $|R_{\text{pp}}|^2$, using Wilheit's radiative transfer model (Wilheit, 1978). These calculated reflectivity values were used to fit the data, although there would be no significant difference obtained if the Fresnel reflectivity was employed.

Equation (15) was used to fit (by a least-squares criterion) the measured backscattering coefficient as a function of incident angle θ. There are four adjustable parameters: σ, l, τ, and η. The first two (i.e., the surface height standard deviation σ and the correlation length l) specify in a statistical manner the geometrical conditions of the soil surface, while the last two (the canopy optical thickness τ and the canopy scattering factor η) describe the characteristics of the vegetation canopy, which is assumed to form a uniform layer over a soil surface.

In applying Eq. (15) to fit the data, one needs to know the 3-dB beamwidth of the antenna pattern. According to Wang (1977), the L-band scatterometer had $\beta \simeq 9°$, and the β value for C-band was approximately $\beta \simeq 2.5°$ (Blanchard, 1983).

Theoretically, any one of the four parameters can be varied to obtain the best fit to the data. However, best fit results show the vegetation backscattering coefficient $\sigma_v^0(\theta)$ is relatively small (although it dominates at angles greater than 30°), and that one can keep τ at a fixed value in fitting the data. This is due to the fact that the τ value for a grass canopy is usually very small and therefore Eq. (2) essentially reduces to the form $\sigma_v^0(\theta) \approx \eta(1 - \tau/\cos\theta)$. Thus good fits to the data can be obtained by varying η, keeping τ fixed.

A previous investigation (Mo, 1982) shows that τ is proportional to the vegetation canopy water content W (kg/m^2) and that it can be given by the simple form

$$\tau = cW, \qquad (17)$$

where c is a frequency-dependent proportionality constant. For L-band, it has been shown that $c \simeq 0.12$ (Mo, 1982). The τ values for C-band are 2–5 times larger than those for L-band. In the present work, the L-band data were fitted by keeping $\tau = 0.06$, which corresponds to an assumption of canopy water content $W = 0.5$ kg/m^2, a typical value for 10–30 cm tall grass (Wang et al., 1980). For C-band, it was assumed that $\tau = 0.12$ for all the cases considered.

With τ fixed at the above values, there are only the three parameters σ, l, and η to be varied to fit the data. Since the wave number k always appears in places where σ or l occurs in the formulas [see Eqs. (6) and (11)], it is convenient to take the dimensionless quantities $k\sigma$ and kl, instead of σ and l, as the adjustable parameters.

Comparisons of some typical best fits (at L- and C-bands) to the data are shown in Figs. 2–5 for the four different grass fields. In these figures, the solid curves represent the calculated backscattering coefficients (dB) for the HH polarization,

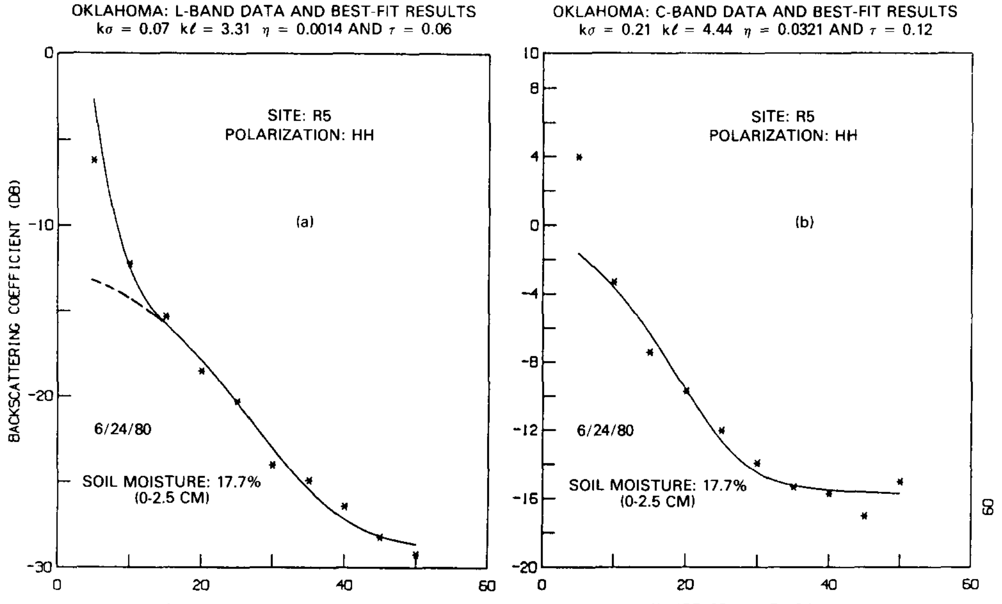

FIGURE 2. Comparison of calculated and measured backscattering coefficients. The asterisks denote the scatterometer data over site R5, and the solid curves represent the calculations obtained with parameters listed at the tops. The dashed curve (at the L-band) would result if the coherent scattering was excluded from the calculation.

and the asterisks denote the data. The parameter values used in the calculations are listed at the top of each figure, and the soil moisture content (wt%) of the 0–2.5 cm surface layer is indicated on the lower part of each figure, together with the date (month/day/year) of the scatterometer measurement.

Figure 2 displays the results for the site R5, which was well managed pasture land (Jackson et al., 1980). The L-band results are shown in part (a), while those for C-band are given in part (b). The model calculations (the solid curves) in Fig. 2 agree well with the observations at all incidence angles, except at 5°, where the scatterometer data probably contain large uncertainties due to instrumental system problems at such near nadir angles (Blanchard, 1983).

The dashed curve in Fig. 2(a) resulted from excluding the coherent backscattering component $\sigma^0_{\mathrm{coh}}(\theta)$. This shows that the coherent scattering makes large contribution at angles near nadir, and its importance can be ignored when the incidence angle is greater than 15°.

The $k\sigma$ value used in obtaining the L-band result as shown in Fig. 2(a) is smaller than that of C-band [Fig. 2(b)] by a factor 3, which is the correct ratio of the k values of C-band to L-band if σ remains constant, as expected. On the other hand, the ratio of the two kl values in Figs. 2(a) and 2(b) does not maintain this 1:3 relationship; thus it implies that the correlation length l, which best describes the surface backscatter is still wavelength-dependent. This indicates that, perhaps, additional parameters are required to specify the soil surface conditions (Allen et al., 1982; Fung and Eom, 1981a).

Figure 3 shows the results for site R6, which was nearly identical to R5 in terms of soil condition and vegetation cover. The best-fit parameter values listed in

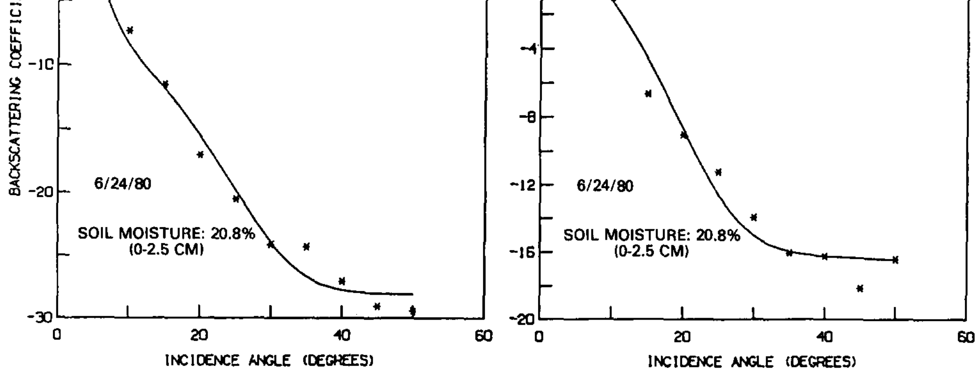

FIGURE 3. Comparison of calculations (solid curves) and scatterometer data (asterisks) taken at L- and C-bands over site R6.

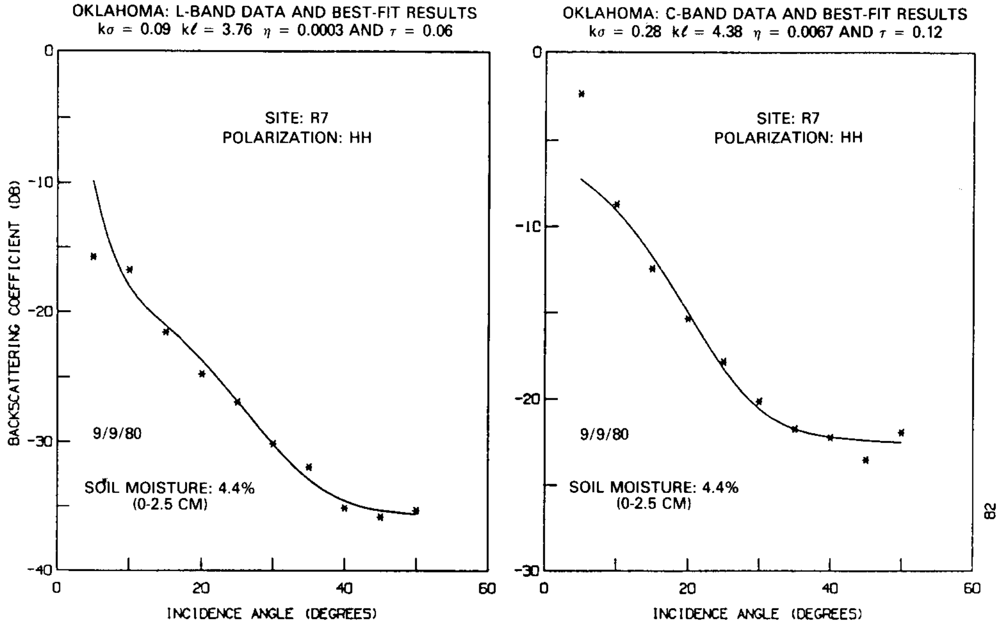

FIGURE 4. Comparison of calculations (solid curves) and scatterometer data (asterisks) taken at L- and C-bands over site R7.

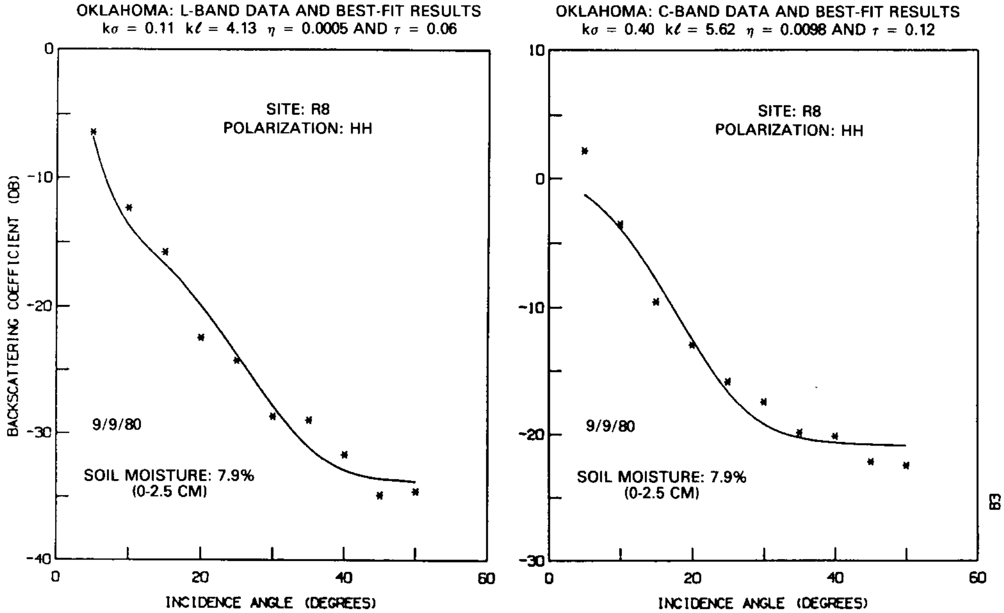

FIGURE 5. Comparison of calculations (solid curves) and scatterometer data taken at L- and C-bands over site R8.

Fig. 3 are comparable to those in Fig. 2, as expected for two nearly identical fields.

Figures 4 and 5 demonstrate the best-fit results and the observations over the two watersheds R7 and R8, which were poorly managed pastures (Jackson et al., 1980; 1982). Hydrologically, sites R7 and R8 were considered identical. The soils (as shown by the soil moistures in Figs. 4 and 5) in both sites were very dry on the experiment date (9 September 1980). The calculated results as shown by the solid curves in Figs. 4 and 5 agree well with the observations, both in magnitude and angular variations. Also, the best-fit $k\sigma$ values (as listed at the top of Figs. 4 and 5) vary with frequency as expected.

Totally, 44 calculations (24 L-band and 20 C-band) and comparisons with the data were performed for the four watersheds from six flights. The best-fit parameter values for all 44 cases are given in Table 1. Those data that are presented in Figs. 2–5 are marked by an asterisk in the first column of Table 1. The last column of Table 1 lists the soil moisture content (wt %) within the 0–2.5 cm surface layer of soil. The average values of the parameters are listed in the bottom row in Table 1.

TABLE 1 Best-Fit Parameters Obtained from Fits to the Scatterometer Data[a]

		L-BAND				C-BAND				SM
DATE	SITE	$k\sigma$	kl	η	τ	$k\sigma$	kl	η	τ	(0–2.5 cm) (wt %)
5/01/78	R5	0.09	2.86	2.3×10^{-3}	0.06	—	—	—	—	21.2
5/12/78		0.14	4.52	3.0×10^{-3}	0.06	0.11	4.73	1.6×10^{-2}	0.12	15.2
5/30/78		0.11	4.40	3.6×10^{-3}	0.06	0.24	5.31	2.8×10^{-2}	0.12	30.1
6/24/80[b]		0.07	3.31	1.4×10^{-3}	0.06	0.21	4.44	3.2×10^{-2}	0.12	17.7
8/14/80		0.08	3.58	0.2×10^{-3}	0.06	0.22	3.74	0.8×10^{-2}	0.12	2.9
9/09/80		0.05	3.24	0.4×10^{-3}	0.06	0.16	4.20	1.0×10^{-2}	0.12	7.9
5/01/78	R6	0.12	4.76	6.7×10^{-3}	0.06	—	—	—	—	22.0
5/12/78		0.22	5.03	2.6×10^{-3}	0.06	0.14	4.89	1.6×10^{-2}	0.12	15.6
5/30/78		0.10	4.15	5.2×10^{-3}	0.06	0.25	4.74	3.1×10^{-2}	0.12	28.4
6/24/80[b]		0.10	4.45	1.7×10^{-3}	0.06	0.26	4.92	2.7×10^{-2}	0.12	20.8
8/14/80		0.13	4.68	0.4×10^{-3}	0.06	0.34	5.14	0.9×10^{-2}	0.12	1.9
9/09/80		0.06	3.90	0.3×10^{-3}	0.06	0.20	4.99	1.0×10^{-2}	0.12	5.6
5/01/78	R7	0.19	3.80	6.1×10^{-3}	0.06	—	—	—	—	19.6
5/12/78		0.14	3.36	4.0×10^{-3}	0.06	0.21	3.05	1.0×10^{-2}	0.12	12.7
5/30/78		0.22	4.67	11.0×10^{-3}	0.06	0.49	5.97	3.8×10^{-2}	0.12	19.9
6/24/80		0.16	3.91	1.6×10^{-3}	0.06	0.40	5.65	2.6×10^{-2}	0.12	15.4
8/14/80		0.16	4.22	0.7×10^{-3}	0.06	0.38	4.71	0.9×10^{-2}	0.12	1.4
9/09/80[b]		0.09	3.76	0.3×10^{-3}	0.06	0.28	4.38	0.7×10^{-3}	0.12	4.4
5/01/78	R8	0.16	3.20	14.3×10^{-3}	0.06	—	—	—	—	22.3
5/12/78		0.14	3.98	8.9×10^{-3}	0.06	0.15	4.20	2.4×10^{-2}	0.12	13.0
5/30/78		0.21	4.79	16.9×10^{-3}	0.06	0.36	5.07	4.4×10^{-2}	0.12	23.5
6/24/80		0.42	6.92	3.1×10^{-3}	0.06	0.45	6.05	3.9×10^{-2}	0.12	16.2
8/14/80		0.17	3.70	1.2×10^{-3}	0.06	0.54	5.06	1.1×10^{-2}	0.12	2.2
9/09/80[b]		0.11	4.13	0.5×10^{-3}	0.06	0.40	5.62	1.0×10^{-2}	0.12	7.9
Average		0.14	4.15	4.0×10^{-3}	0.06	0.29	4.84	2.1×10^{-2}	0.12	

[a] Note that the value of $\tau = 0.06$ is fixed for L-band and $\tau = 0.12$ for C-band. The last column gives the soil moisture (SM) within the 0–2.5 cm surface layer. The average values of these parameters are listed in the bottom row.

[b] Data are shown in Figs. 2–5, respectively.

Table 1 shows that the surface parameters for sites R5 and R6 have approximately the same numerical values, and that those for R7 and R8 are also similar. Generally, the $k\sigma$ values for R7 and R8 are larger than those of R5 and R6. This is in agreement with the fact that the soil surfaces of sites R7 and R8 were more highly eroded and therefore were rougher than those of R5 and R6 (Jackson et al., 1980; 1982).

Discussion

The surface parameter values (for the same site) given in Table 1 show some variations from one day to another in the same year. It is possible that this is due to the fact the surface conditions changed during the period of data acquisition. However, another possible explanation is that the apparent variation in the best fit parameters might be due to small errors in absolute calibration of the scatterometer system from one flight to another.

To investigate this possibility, we made some studies of the backscattering coefficient sensitivity to the parameters for L-band. The results are given in Table 2, which lists the best-fit parameters values that would result, if the measured backscattering coefficients, $\sigma^0(\theta)$, were arbitrarily increased by 2 dB and 5 dB, respectively, at all angles.

Comparison of results in Tables 1 and 2 reveals that in the case of $\sigma^0(\theta)+5$ dB, the $k\sigma$ values (in Table 2) are approximately 2 times larger than the corresponding ones in Table 1, and that the $\sigma^0(\theta)+2$ dB case requires about a 50% increment in the surface parameter values. Therefore, if the soil surface conditions of the sites remained the same during the data taking period, particularly for the same year, the apparent variations in the best-fit parameter value (in Table 1) can be attributed to small errors of the scatterometer system from one flight to the other. Also an assumption of ±2 dB errors in the measured angular distributions of the backscattering coefficient would adequately account for the range of variation in the parameter values as given in Table 1. The η values (C-band)

TABLE 2 Best-Fit Parameters (L-Band) Obtained from Fits for the Cases of $\sigma^0(\theta)+2$ dB, and $\sigma^0(\theta)+5$ dB, Respectively[a]

		$\sigma^0(\theta)+2$ dB				$\sigma^0(\theta)+5$ dB				SM (0–2.5 cm)
DATE	SITE	$k\sigma$	kl	η	τ	$k\sigma$	kl	η	τ	(wt %)
5/01/78	R5	0.11	3.48	5.7×10^{-3}	0.06	0.17	3.89	1.3×10^{-2}	0.06	21.2
5/12/78		0.24	6.44	6.4×10^{-3}	0.06	0.39	7.53	1.3×10^{-2}	0.06	15.2
5/30/78		0.17	5.25	6.8×10^{-3}	0.06	0.26	5.75	1.4×10^{-2}	0.06	30.1
5/01/78	R6	0.17	5.73	12.0×10^{-3}	0.06	0.27	6.37	2.5×10^{-2}	0.06	22.0
5/12/78		0.36	6.38	4.9×10^{-3}	0.06	0.56	7.21	0.9×10^{-2}	0.06	15.6
5/30/78		0.14	4.80	9.3×10^{-3}	0.06	0.22	5.27	2.0×10^{-2}	0.06	28.4
5/01/78	R7	0.29	4.92	13.9×10^{-3}	0.06	0.41	5.06	2.6×10^{-2}	0.06	19.6
5/12/78		0.18	3.43	6.5×10^{-3}	0.06	0.26	3.55	1.3×10^{-2}	0.06	12.7
5/30/78		0.35	6.17	21.2×10^{-3}	0.06	0.51	6.56	4.1×10^{-2}	0.06	19.9
5/01/78	R8	0.21	3.67	28.1×10^{-3}	0.06	0.31	3.95	5.9×10^{-2}	0.06	22.3
5/12/78		0.18	4.22	14.6×10^{-3}	0.06	0.26	4.44	2.9×10^{-2}	0.06	13.0
5/30/78		0.30	5.69	29.7×10^{-3}	0.06	0.44	6.06	5.8×10^{-2}	0.06	23.5

[a] As explained in the text. Note that $\tau = 0.06$ was used in all cases.

in Table 1 are comparable to results reported by other investigators (Attema et al., 1978) at the 8.6 GHz frequency for a wheat field, which is assumed to be structurally similar to the grass in the pasture.

In addition to the soil surface conditions and the vegetation parameters as discussed in the previous section, soil moisture content also has a large effect on the backscattering coefficient. Figure 6 demonstrates some of the calculated results of $\sigma^0(\theta)$ as a function of volumetric soil moisture (SM) at the five incidence angles of 10°, 20°, 30°, 40°, and 50°, as labeled on the curves. These results for L- and C-band were calculated with the average values of the best-fit parameters, as given in the bottom row of Table 1.

Figure 6 shows that the backscattering coefficient increases with SM. Its increment in low SM region is faster than that at high SM (> 30%). Below SM = 30%, the $\sigma^0(\theta)$ values in Fig. 6 vary approximately linearly with SM. Linear regression analysis of $\sigma^0(\theta)$ values below SM = 30% was performed, and the results are listed in Table 3, which contains the values of intercept and slope for each incidence angle.

Table 3 shows that the backscattering coefficient sensitivity to soil moisture, defined as $d\sigma^0(\theta)/d\mathrm{SM}$ (which equals to the slope of the regression line), decreases

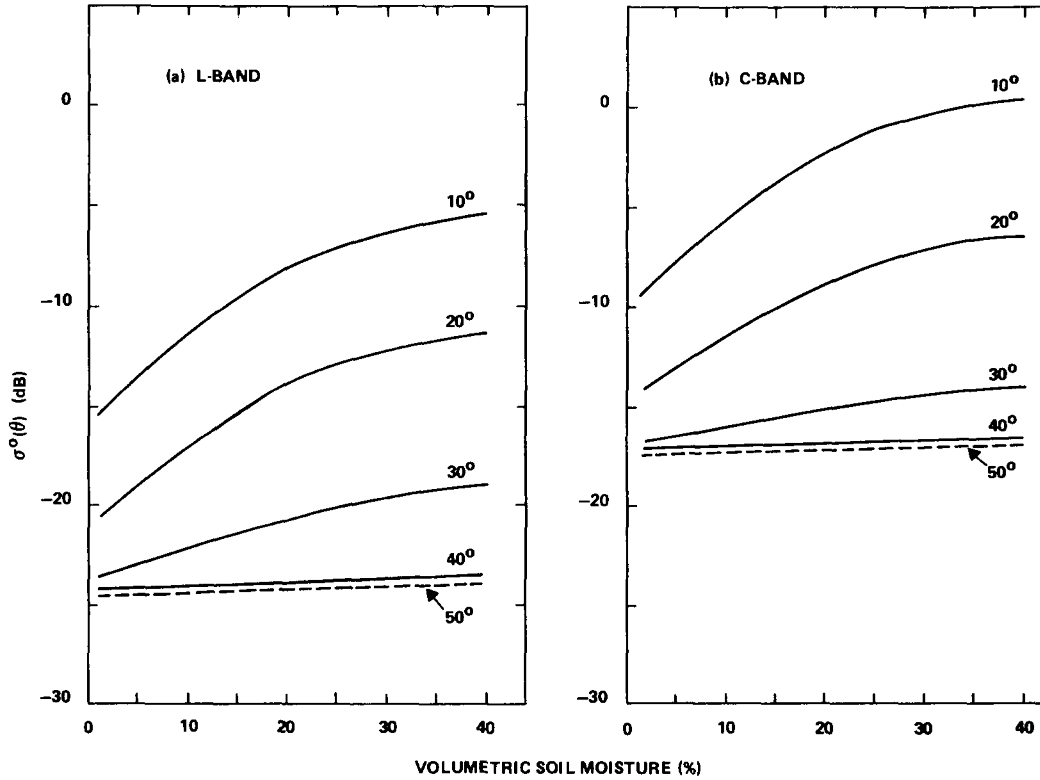

FIGURE 6. Backscattering coefficients (at fixed incidence angle) versus volumetric soil moistures. These results were calculated using the average parameters as listed in the bottom row in Table 1, and the ground was assumed to have uniform profiles of soil moisture and a temperature of 293°K: (a) L-band, (b) C-band.

TABLE 3 Linear Regression Results of Backscattering Coefficient versus Volumetric Soil Moisture (< 30%), at Different Incident Angles θ

	L-Band		C-Band	
θ(°)	Intercept	Slope	Intercept	Slope
5	−9.5	0.32	−6.5	0.32
10	−14.9	0.31	−9.5	0.31
15	−17.4	0.30	−12.0	0.28
20	−19.9	0.27	−14.6	0.24
25	−22.2	0.22	−16.4	0.16
30	−23.6	0.14	−17.2	0.07
35	−24.1	0.06	−17.4	0.03
40	−24.3	0.02	−17.4	0.01
45	−24.3	0.00	−17.5	0.00
50	−24.4	0.00	−17.6	0.00

as the incidence angle θ increases. At $\theta > 40°$, Table 3 shows the slope values are almost zero [i.e., $d\sigma^0(\theta)/d\mathrm{SM} \approx 0$]. This is due to the fact that the vegetation scattering appears to be the primary contributor to the backscattering coefficient at large angles. In obtaining the results as shown in Fig. 6, it was assumed that the factor η is independent of the soil moisture. In practice, the factor η varies as a function of vegetation canopy water content, which is highly dependent on the soil moisture (see Table 1); therefore, the slope values of measured backscattering coefficients at large angles may differ than those shown in Fig. 6. The slope values in Table 3 are in good agreement with the results reported by Ulaby et al. (1981).

Table 3 also shows that the slopes for both L- and C-band are relatively con-

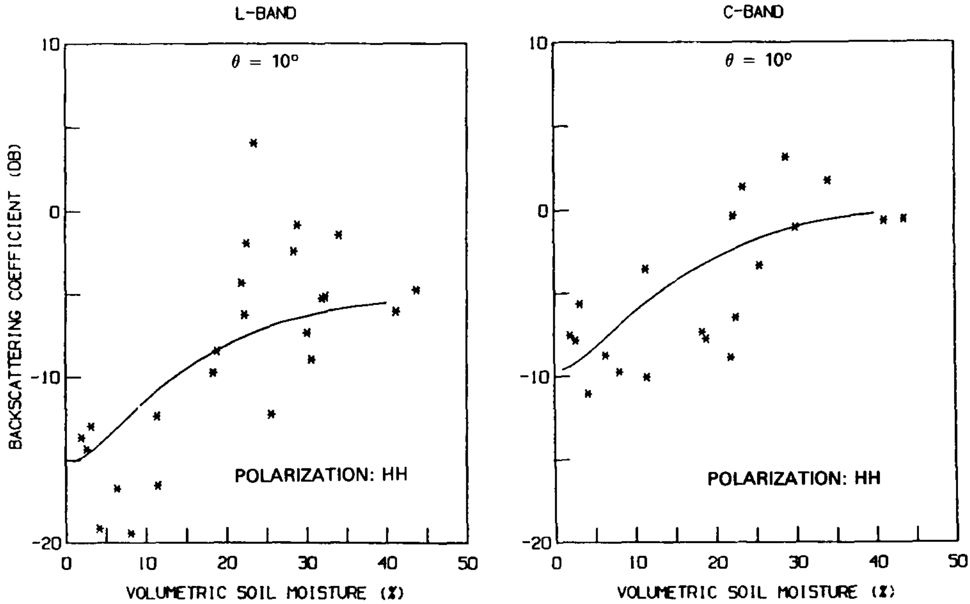

FIGURE 7. Comparison of calculated and measured backscattering coefficients at $\theta = 10°$.

stant up to 20°, but that the intercept changes by about 10 dB in L-band and 8 dB in C-band.

Figure 7 shows the comparison of the calculated backscattering coefficients and the scatterometer data at $\theta = 10°$, as a function of volumetric soil moisture. The calculated results (solid curves) are the same as shown in Fig. 6, and the data (asterisks) are plotted as a function of the soil moisture within the surface 0–2.5 cm of soil depth. Figure 7 demonstrates that the agreement between the calculations and data is reasonably good within experimental errors.

Conclusions

We have shown that the measured angular distribution of backscattering coefficient of vegetation-covered fields can be satisfactorily reproduced, using the model developed in this study. The model takes into consideration both coherent and incoherent scattering from rough soil surfaces. In addition, the vegetation scattering is also included in the model and it appears to be dominant at large incident angles (i.e., $\theta > 30°$). The coherent scattering component, which is very important at angles near nadir, is introduced into the model through the antenna gain pattern with finite 3-dB beamwidth. The incoherent scattering, which vanishes for a smooth soil surface, contributes to the backscattering coefficient at all incident angles for rough soil surfaces.

The $k\sigma$ values obtained from best fits to scatterometer data of various sites qualitatively correlate with the degree of roughness of the soil surfaces. Also, the frequency dependence of the best-fit $k\sigma$ values is in agreement with expectation in most cases (i.e., the values at C-band are about 3 times the value at L-band). This implies that, by least-squares fit to the scatterometer data, it may be possible to obtain reliable value of the standard deviation of a rough surface. However, the kl values do not scale properly with wavelength. This result may imply that σ and l are not adequate descriptors of the surface roughness. More study of this problem is required.

We would like to thank Drs. Bruce Blanchard and James Wang for discussions concerning the operations of the scatterometers.

References

Allen, C. T., Ulaby, F. T., and Fung, A. F. (1982), A model for the radar backscattering coefficient of bare soil, University of Kansas Center for Research, Inc., Lawrence, RSL TR 460-8 (AgRISTARS SM-K1-04181).

Attema, E. P. W., and Ulaby, F. T. (1978), Vegetation modeled as a water cloud, *Radio Sci.* 13(2):357–364.

Blanchard, B. (1983), personal communication.

Eom, H. J., and Fung, A. K. (1982), Scattering coefficients of Kirchhoff surfaces with Gaussian and non-Gaussian surface statistics, University of Kansas Center for Research, Inc., Lawrence, RSL TR 4601-2 (AgRISTARS SM-K2-04370).

Fung, A. K., and Eom, H. J. (1981a), An approximate model for backscattering and emission from land and sea, paper presented at the International Geoscience and Remote Sensing Symposium, IEEE Geoscience and Remote Sensing Society, Washington, D.C., June (also TR SM-K1-0409, Remote Sensing Laboratory, University of Kansas).

Fung, A. K., and Eom, H. J. (1981b), Note on the Kirchhoff rough surface solution in backscattering, *Radio Sci.* 16:299–302.

Jackson, T. J. (1983), Preliminary analysis of aircraft radar data collected at Chickasha, Oklahoma, 1978–1980, USDA Hydrology Laboratory, Beltsville, Maryland, Technical Report.

Jackson, T. J., Schmugge, T. J., Coleman, G. C., Richardson, C., Chang, A., Wang, J., and Engman, E. T. (1980), Aircraft remote sensing of soil moisture and hydrologic parameters, Chickasha, Oklahoma, and Riesel, Texas, 1978 Data Report, ARR-NE-8, USDA, Beltsville, Maryland.

Jackson, T. J., O'Neill, P., Coleman, G. C., and Schmugge, T. J. (1982), Aircraft remote sensing of soil moisture and hydrologic parameters, Chickasha, Oklahoma, 1980 Data Report, USDA, Beltsville, Maryland.

Mo, T. (1982), Incoherent scattering of microwave radiation from rough soil surfaces, Computer Sciences Corporation, Silver Spring, Maryland, CSC/TR-82/6001 (AgRISTARS SM-G2-04291).

Mo, T., Choudhury, B. J., Schmugge, T. J., Wang, J. R., and Jackson, T. J. (1982), A model for microwave emission from vegetation-covered fields, *J. Geophys. Res.* 87:11229–11237.

Semyonov, B. (1966), Approximate computation of scattering of electromagnetic waves by rough surface contours, *Radio Eng. Electron. Phys.* 11:1179–1187.

Stogryn, A. (1967), Electromagnetic scattering from rough finitely conducting surfaces, *Radio Sci.* 2:415–428.

Theis, S. W., McFarland, M. J., Rosenthal, W. D., and Jones, C. L. (1982a), Microwave remote sensing of soil moistures, Technical Report RSC-3458-129, Remote Sensing Center, Texas A&M University, College Station, Texas.

Theis, S. W., McFarland, M. J., Rosenthal, W. D., and Jones, C. L. (1982b), Measurement of soil moisture trends with airborne scatterometers, Technical Report RSC-3458-131, Remote Sensing Center, Texas A&M University, College Station, Texas.

Tsang, L., and Newton, R. W. (1982), Microwave emission from soils with rough surfaces, *J. Geophys. Res.* 11:9017–9024.

Tsang, L., Blanchard, A. J., Newton, R. W., and Kong, J. A. (1982), A simple relation between active and passive microwave remote sensing measurements of earth terrain, *IEEE Trans. Geosci. Remote Sens.* GE-20:482–485.

Ulaby, F. T., Batlivala, P. P., and Dobson, M. C. (1978), Microwave backscatter dependence on surface roughness, soil moisture and soil texture: Part I—bare soil, *IEEE Trans. Geosci. Electron.* GE-16:286–295.

Ulaby, F. T., Bradley, G. A., and Dobson, M. C. (1981), Microwave backscatter dependence on surface roughness, soil moisture and soil texture: Part II—vegetation covered soil, *IEEE Trans. Geosci. Electron.* GE-19:33–40.

Ulaby, F. T., Moore, R. K., and Fung, A. K. (1982), *Microwave Remote Sensing: Active and Passive*, Vol. 2, Addison-Wesley, Reading, Massachusetts.

Wang, J. R. (1977), A model of the 1.6 GHz scatterometer, Lockheed Electronics Company, Houston, Texas, Job Order 75-415 (NASA/Johnson Space Center JSC-12990).

Wang, J. R., Shiue, J., Engman, E., McMurtrey, J., Lawless, P., Schmugge, T., Jackson, T., Gould, W., Fuchs, J., Calhoon, C., Carnahan, T., Hirschmann, E., and Glazar, W. (1980), Remote Measurements of Soil Moisture by Microwave Radiometers at BARC Test Site, NASA Technical Memorandum 80720.

Wilheit, T. T. (1978), Radiative transfer in a plane stratified dielectric, *IEEE Trans. Geosci. Electron.* GE-16:138–143.

Received 26 April 1983; revised 3 October 1983.